

# Environmental Science Processes & Impacts

Accepted Manuscript



This is an *Accepted Manuscript*, which has been through the Royal Society of Chemistry peer review process and has been accepted for publication.

*Accepted Manuscripts* are published online shortly after acceptance, before technical editing, formatting and proof reading. Using this free service, authors can make their results available to the community, in citable form, before we publish the edited article. We will replace this *Accepted Manuscript* with the edited and formatted *Advance Article* as soon as it is available.

You can find more information about *Accepted Manuscripts* in the [Information for Authors](#).

Please note that technical editing may introduce minor changes to the text and/or graphics, which may alter content. The journal's standard [Terms & Conditions](#) and the [Ethical guidelines](#) still apply. In no event shall the Royal Society of Chemistry be held responsible for any errors or omissions in this *Accepted Manuscript* or any consequences arising from the use of any information it contains.



[rsc.li/process-impacts](http://rsc.li/process-impacts)

## Environmental impact

In this study, we examined the relationships between different exposure metrics (MC, NC, and active SAC) for different nanoparticles in workplaces, using multiple evaluation indices: concentration ratio (CR, activity: background), exposure ranking (ER), between-metric correlation coefficients (R), ratio of cumulative percentage by number (APN), and cumulative percentage by mass (APM). Real-time  $NC_{20-1000nm}$ , active  $SAC_{10-1000nm}$ , and respirable  $MC_{100-1000nm}$ , were determined for different nanoparticles including engineered nanoparticles (i.e. ferric oxide (Nano- $Fe_2O_3$ ) and alumina (Nano- $Al_2O_3$ ), and ultrafine particles (i.e. welding particles, diesel exhaust, and grinding-wheel dust). The CR, ER, and correlation coefficients (R) were used to analyze the relationships between the three real-time concentration metrics. The number (10~469.8 nm) and mass (10-560 nm) size distributions of Nano- $Al_2O_3$  and grinding-wheel dust were measured using a scanning mobility particle sizer and cascade impactor, respectively. The ratio of cumulative percentage by number (APN) and cumulative percentage by mass (APM) was used to analyze whether nanoparticle number is predominant, as compared with nanoparticle mass.

1  
2  
3  
4  
5  
6  
7  
8  
9  
10  
11  
12  
13  
14  
15  
16  
17  
18  
19  
20  
21  
22  
23  
24  
25  
26  
27  
28  
29  
30  
31  
32  
33  
34  
35  
36  
37  
38  
39  
40  
41  
42  
43  
44  
45  
46  
47  
48  
49  
50  
51  
52  
53  
54  
55  
56  
57  
58  
59  
60

## Relationships between number, surface area, and mass concentrations of different nanoparticles in workplaces

Hua Zou <sup>a</sup>, Qunwei Zhang <sup>b</sup>, Mingluan Xing <sup>a</sup>, Xiangjing Gao <sup>a</sup>, Lifang Zhou <sup>a</sup>, David J Tollerud <sup>b</sup>, Shichuang Tang <sup>c\*</sup>, Meibian Zhang <sup>a\*\*</sup>

### Abstract

No consistent metric for measuring exposure to nanoparticles has yet been agreed upon internationally. This study seeks to examine the relationship between number concentration (NC), surface area concentration (SAC), and mass concentration (MC) of nanoparticles in workplaces. Real-time  $NC_{20-1000nm}$ ,  $SAC_{10-1000nm}$ , and respirable  $MC_{100-1000nm}$  were determined for different nanoparticles. Concentration ratio (CR, activity: background), exposure ranking (ER), and between-metric correlation coefficients (R) were used to analyze the relationships between the three metrics. The ratio of cumulative percentage by number (APN) and cumulative percentage by mass (APM) was used to analyze whether nanoparticle number is predominant, as compared with nanoparticle mass. The CRs of  $NC_{20-1000nm}$  and  $SAC_{10-1000nm}$  for different nanoparticles at the corresponding work sites were higher than those of respirable  $MC_{100-1000nm}$ . The ERs of  $NC_{20-1000nm}$  for nano- $Fe_2O_3$  and nano- $Al_2O_3$  were the same as those of  $SAC_{10-1000nm}$ , but were inconsistent with those of respirable  $MC_{100-1000nm}$ . The order of correlation coefficients between  $NC_{20-1000nm}$ ,  $SAC_{10-1000nm}$ , and respirable  $MC_{100-1000nm}$  was:  $R_{SAC \text{ and } NC} > R_{SAC \text{ and } MC} > R_{NC \text{ and } MC}$ . The ratios of APN and APM for nano- $Al_2O_3$  and grinding-wheel particles (less than 100 nm) at the same work site were 2.03 and 1.65, respectively. NC and SAC metrics are significantly distinct from MC in characterizing exposure to airborne nanoparticles. Simultaneous measurement of NC, SAC, and MC should be conducted as part of nanoparticle exposure assessment strategies and

1  
2  
3  
4 epidemiological studies.

5  
6 **Keywords:** Nanoparticles; Exposure metric; Exposure assessment; Workplace  
7  
8  
9

## 10 11 **Introduction**

12  
13  
14 Nanoparticles, or ultrafine particles, are defined as particles with nominal diameters (such as  
15  
16 geometric, aerodynamic, mobility-related, and projected-area diameters) of less than 100 nm. <sup>1</sup>

17  
18 The term nanomaterial refers to any material having one or more external dimensions (or an  
19  
20 internal structure) on the nanoscale, such that it exhibits novel characteristics compared to its  
21  
22 counterparts without nanoscale features. <sup>2</sup> Nanoparticles (engineered nanoparticles and ultrafine  
23  
24 particles) in the workplace are formed through nucleation or evaporation (condensation), usually  
25  
26 originating from four potential sources: hot processes (e.g. welding and metal smelting);  
27  
28 combustion (e.g. diesel and gasoline engines); mechanical processes (e.g. high-speed grinding and  
29  
30 high-energy drilling); and the production, handling, and use of nanomaterials. <sup>1,3</sup> Recently,  
31  
32 concerns have been raised about the potential health risks posed by engineered nanoparticles  
33  
34 having such novel characteristics as small size, high surface area, and high surface reactivity. <sup>4-7</sup>  
35  
36 Ultrafine particles, as a critical component of ambient fine particles, may contribute to the  
37  
38 occurrence of cardiovascular or pulmonary diseases caused by fine particle exposure. <sup>8-12</sup>  
39  
40  
41  
42  
43  
44  
45

46  
47 The choice of appropriate exposure metrics is critical for dose–effect assessment of  
48  
49 nanoparticles. To date, there is no international consensus on the choice of exposure metrics. <sup>6</sup>

50  
51 Mass concentration (MC) is a traditional metric for establishing occupational exposure limits for  
52  
53 particles. However, *in vitro* and *in vivo* studies have shown that MC does not accurately reflect the  
54  
55 toxicological effect induced by engineered nanoparticles, owing to the latter's unique  
56  
57  
58  
59  
60

1  
2  
3  
4 physico-chemical properties.<sup>13</sup>  
5

6 In contrast, number concentration (NC) and surface area concentration (SAC) have shown a  
7  
8 good dose–effect relationship in terms of oxidative stress and inflammatory responses in the  
9  
10 lungs.<sup>8,14-16</sup> The unique characteristics of ultrafine particles—including high number count and  
11  
12 large surface area per unit of mass, small size, and surface reactivity—are considered to play  
13  
14 important roles in adverse health effects.<sup>5,17</sup> Based on these findings, NC and SAC can therefore  
15  
16 be considered appropriate for assessing particle toxicity.  
17  
18  
19

20  
21 There is a need for NC, SAC, and MC to be applied simultaneously in field exposure studies,  
22  
23 as well as to investigate whether or not these metrics are correlated to occupational exposure  
24  
25 scenarios. At present, there are a few documents available to evaluate different exposure metrics  
26  
27 for characterizing nanoparticles in workplaces.<sup>18,19</sup> Recent studies indicate the following: (1) a  
28  
29 possible correlation between different metrics has been identified; in terms of ultrafine particles in  
30  
31 workplaces, SAC appears to show a strong correlation with NC and a weak correlation with  
32  
33 respirable MC.<sup>20-22</sup> However, for engineered nanoparticles, the correlation between NC and MC is  
34  
35 not always consistent, and data on SAC are insufficient;<sup>18</sup> (2) the exposure rankings of  
36  
37 occupational groups exposed to ultrafine particles are quite different, but previous results were  
38  
39 shown to be highly dependent on the chosen exposure metrics;<sup>21,23</sup> and (3) nanoparticles  
40  
41 frequently account for only a small fraction of total mass concentration, but account for a high  
42  
43 cumulative percentage of total number concentration.<sup>13,20,22,24</sup> Furthermore, real-time NC, SAC,  
44  
45 and respirable MC can be determined using commercial measuring instruments that are practical,  
46  
47 economical, and portable for most workplace monitoring situations and that may aid in timely  
48  
49 identification of particle sources or “hot spots”. Real-time NC and lung deposited or active SAC  
50  
51  
52  
53  
54  
55  
56  
57  
58  
59  
60

1  
2  
3  
4 measurements determined by portable monitoring instruments may be affected by particle  
5  
6 diameter (dp), particle morphology and charging efficiencies. Lung deposited surface area per  
7  
8 particle in a size range from 20 to 400 nm is proportional to  $dp^{1.13, 25, 26}$ . The size dependences of  
9  
10 number and mass per particle are  $dp^0$  and  $dp^3$ , respectively. NC is inversely proportional to  $dp^3$  per  
11  
12 mass unit based on the formula (i.e.  $NC=6/\pi\rho dp^3 \times MC$ ). Active SAC is proportional to  $dp^2$  when  
13  
14 dp is much smaller than the mean free path ( $\lambda$ , 66 nm for air at standard temperature and pressure)  
15  
16 of surrounding gas, however, active SAC increases proportionally to dp when dp increases.<sup>20,27-29</sup>  
17  
18  
19

20  
21 In this study, we examined the relationships between different exposure metrics (MC, NC,  
22  
23 and lung deposited SAC) for different nanoparticles in workplaces, using multiple evaluation  
24  
25 indices: concentration ratio (CR, activity: background), exposure ranking (ER), between-metric  
26  
27 correlation coefficients (R), ratio of cumulative percentage by number (APN), and cumulative  
28  
29 percentage by mass (APM). The definitions of these terms and their implications are given in  
30  
31 Table 1. Real-time  $NC_{20-1000nm}$ , lung deposited  $SAC_{10-1000nm}$ , and respirable  $MC_{100-1000nm}$ , were  
32  
33 determined for different nanoparticles including engineered nanoparticles (i.e. ferric oxide  
34  
35 (Nano- $Fe_2O_3$ ) and alumina (Nano- $Al_2O_3$ ), and ultrafine particles (i.e. welding particles, diesel  
36  
37 exhaust, and grinding-wheel dust). The CR, ER, and correlation coefficients (R) were used to  
38  
39 analyze the relationships between the three real-time concentration metrics. The number  
40  
41 (10~469.8 nm) and mass (10-560 nm) size distributions of Nano- $Al_2O_3$  and grinding-wheel dust  
42  
43 were measured using a scanning mobility particle sizer and cascade impactor, respectively. The  
44  
45 ratio of cumulative percentage by number (APN) and cumulative percentage by mass (APM) was  
46  
47 used to analyze whether nanoparticle number is predominant, as compared with nanoparticle  
48  
49 mass.  
50  
51  
52  
53  
54  
55  
56  
57  
58  
59  
60

## Methods

### Description of workplace

Five factories in Zhejiang Province, East China, were selected for the field investigation. The five factories include two nanomaterial manufacturers at which there might be occupational exposure to Nano-Fe<sub>2</sub>O<sub>3</sub> and Nano-Al<sub>2</sub>O<sub>3</sub>, and three non-nanomaterial manufacturers (kitchenware, elevator, and foundry) that generate ultrafine particles as by-products. Nano-Fe<sub>2</sub>O<sub>3</sub> ( $\alpha$ -Fe<sub>2</sub>O<sub>3</sub>) particles were produced by chemical synthesis. The production processes are described briefly as follows: (1) oxidation reaction of FeSO<sub>4</sub> solution; (2) colloid preparation for ferric hydroxide (Fe(OH)<sub>3</sub>); (3) synthesis reaction with a part of the Fe<sub>2</sub>(SO<sub>4</sub>)<sub>3</sub> solution, the Fe(OH)<sub>3</sub> colloid, H<sub>2</sub>SO<sub>4</sub>, and an iron sheet; (4) surface treatment of  $\alpha$ -Fe<sub>2</sub>O<sub>3</sub>·nH<sub>2</sub>O crystals using a water-soluble anionic polymer; (5) flash evaporation of wet product of  $\alpha$ -Fe<sub>2</sub>O<sub>3</sub>·nH<sub>2</sub>O in a flash dryer; (6) powder screening: a portion of the  $\alpha$ -Fe<sub>2</sub>O<sub>3</sub>·nH<sub>2</sub>O product is manually spread onto a flat plate; (7) calcinations: the  $\alpha$ -Fe<sub>2</sub>O<sub>3</sub> product is produced by removing crystal water from  $\alpha$ -Fe<sub>2</sub>O<sub>3</sub>·nH<sub>2</sub>O in an infrared dryer; (8) material feeding: the  $\alpha$ -Fe<sub>2</sub>O<sub>3</sub> material is manually fed into a semi-open container for washing; (9)  $\alpha$ -Fe<sub>2</sub>O<sub>3</sub> or  $\alpha$ -Fe<sub>2</sub>O<sub>3</sub>·nH<sub>2</sub>O packaging. At the Nano-Fe<sub>2</sub>O<sub>3</sub> manufacturer site, three work sites (for packaging, powder screening, and material feeding, respectively) were selected as sampling locations, on the basis that there might be airborne nanoparticles generated there (Table 2).

The production process at the Nano-Al<sub>2</sub>O<sub>3</sub> manufacturer can be summarized as follows: (1) grinding of large-size AlCl<sub>3</sub> particles in a closed container; (2) manual feeding of AlCl<sub>3</sub> into a reactor; (3) chemical reaction in a reactor using gas phase method; (4) manual sampling of semi-product for quality testing; (5) separation of HCL gas and Nano-Al<sub>2</sub>O<sub>3</sub> particles via

1  
2  
3  
4 air-blowing in a separator; and (6) automatic packaging. Three work sites were selected as  
5  
6 sampling locations: the packaging area, control room, and a cold air inlet at the junction of the  
7  
8 reactor and separator (Table 2). Three single work sites in the other three factories were selected to  
9  
10 investigate workplace exposure to ultrafine particles: forklift operation (kitchenware  
11  
12 manufacturer), gas metal arc welding (GMAW) for part jointing (elevator manufacturer), and  
13  
14 casting polishing (foundry) (Table 2). Outdoor background particulates served as controls for the  
15  
16  
17  
18  
19 five types of nanoparticles.

### 20 21 **Monitoring and sampling system**

22  
23  
24 Table 3 provides details of the monitoring and sampling system. The real-time monitoring  
25  
26 system measured total particle concentrations (number, mass, and surface area) and size  
27  
28 distribution by number. The membrane-based sampling system was used to collect airborne  
29  
30 nanoparticles and to analyze their elemental compositions.

31  
32  
33  
34 Total NC was determined using a P-Trak ultrafine particle counter (Model 8525, TSI, USA).  
35  
36 The counter is a portable condensation particle counter (CPC) calibrated by the manufacturer, and  
37  
38 was set to zero daily prior to sampling. It counts particles enlarged in a saturated vapor  
39  
40 environment using optical sensing. The isopropyl alcohol cartridge was replaced every 5.5 h. Total  
41  
42 or respirable MC was measured using a real-time aerosol monitor (DustTrak 8530, TSI, USA),  
43  
44 which is a portable laser-scattering photometer. The monitor was calibrated by the manufacturer to  
45  
46 the respirable fraction. Before sampling, a high-efficiency particulate absorption (HEPA) filter  
47  
48 was used to confirm that the monitor reading was zero. Lung deposited SAC was determined  
49  
50 using a surface area monitor (Aero Trak™ 9000, TSI, USA). The monitor, which consists of a  
51  
52 diffusion charger and an electrometer, was used in alveolar deposition mode. Based on the  
53  
54  
55  
56  
57  
58  
59  
60

1  
2  
3  
4 International Commission on Radiological Protection's lung deposition model for a reference  
5  
6 worker with specific physiological and activity-related parameters, the amount of charge on  
7  
8 particles charged with unipolar positive ions by diffusion is proportional to the surface area of  
9  
10 lung-deposited particles.<sup>30</sup> Comparisons were made between monitors used and corresponding  
11  
12 reference monitors of the same kind. The latter were newly purchased and were calibrated by the  
13  
14 manufacturers. The relative measurement error, i.e.  $(\text{value}_{\text{measurement}} - \text{value}_{\text{reference}}) / \text{value}_{\text{reference}} \times$   
15  
16 100%, serves as an indicator for assessing the comparability of monitors used. In this study,  
17  
18 relative measurement errors of these real-time monitors were less than 5%.  
19  
20  
21  
22  
23

24 Size distribution by number was determined using a scanning mobility particle sizer (SMPS,  
25  
26 Model 3034, TSI, USA). The SMPS contains a differential mobility analyzer (DMA) and a CPC  
27  
28 that can determine particle size distribution by number of nanoparticles based on  
29  
30 electrical-mobility diameters. The instrument was calibrated based on the manufacturer's  
31  
32 instructions.  
33  
34  
35

36 The morphologies and elemental compositions of nanoparticles were analyzed using  
37  
38 scanning electron microscopy (SEM, S4800, HITACH, Japan) and energy-dispersive X-ray  
39  
40 spectroscopy (EDX, S4800, HITACH, Japan), respectively. Airborne particles in workplaces were  
41  
42 collected on the aluminum filter using a cascade impactor (Nano-MOUDI, 125A, MSP, USA).  
43  
44 The impactor has 13 stages corresponding to cut sizes of 10000 nm, 5600 nm, 3200 nm, 1800 nm,  
45  
46 1000 nm, 560 nm, 320 nm, 180 nm, 100 nm, 56 nm, 32 nm, 18 nm, and 10 nm, respectively. The  
47  
48 mass concentrations of particle sizes smaller than 560 nm (in terms of aerodynamic diameter ( $D_a$ ))  
49  
50 were merged into four size classifications: 10~, 56~, 100~, and 320~560 nm. Particle number  
51  
52 concentrations at different sizes of electrical mobility diameter ( $D_p$ ) were determined by the SMPS  
53  
54  
55  
56  
57  
58  
59  
60

and were also merged into four size classifications, i.e. 10~, 54.2~, 96.5~, and 327.8~469.8 nm for nano-Al<sub>2</sub>O<sub>3</sub> and 10~, 35.2~, 62.5~, 198.1~ 352.3 nm for grinding-wheel dust, respectively (Table 7). D<sub>p</sub> was converted to the D<sub>a</sub> through the following equation:<sup>31</sup>

$$D_a = \frac{D_p}{\sqrt{\frac{\chi \rho_0}{\rho_p}}} \quad (\text{Eq. 1})$$

where D<sub>a</sub> and D<sub>p</sub> are aerodynamic and mobility diameters, respectively; ρ<sub>0</sub> is the reference density (1 g/cm<sup>3</sup>); ρ<sub>p</sub> is the density of the particle. The density of nano-Al<sub>2</sub>O<sub>3</sub> is 1.24 g/cm<sup>3</sup>, as provided by the nanomaterial manufacturer; the density of grinding-wheel particles is about 2.62 g/cm<sup>3</sup>, based on a standard in China regarding the conversion method between relative mass concentration and mass concentration of dust in workplaces (TB/T2323-1992); χ is the shape factor (1), assuming spherical shape for primary nanoparticles. Thus Eq. 1 becomes:

$$D_a = D_p \times 1.11 \quad (\text{aerodynamic diameter for nano-Al}_2\text{O}_3) \quad (\text{Eq. 2})$$

$$D_a = D_p \times 1.62 \quad (\text{aerodynamic diameter for grinding-wheel particles}) \quad (\text{Eq. 3})$$

Consequently, the size ranges of 10~469 nm and 10~352.3 nm in D<sub>p</sub> for measuring nano-Al<sub>2</sub>O<sub>3</sub> and grinding-wheel dust, respectively, were converted to 11.1~521.5 nm and 16.2~570.7 nm in D<sub>a</sub>, similar to the values of 10~560 nm in D<sub>a</sub> determined using Nano-MOUDI. This allowed comparison of the cumulative percentage by mass (APM) and the cumulative percentage by number (APN) at similar size ranges.

### Sampling or testing strategy

The sampling process lasted three days at each factory (from October 2012 to May 2013). The sampling or testing protocol was as follows: (1) walkthrough survey: an observational walkthrough survey of the production areas and processes was conducted to identify potential sources of particle emission. A CPC was used to trace the major emission sources of nanoparticles;

1  
2  
3 (2) background measurements: outdoor or indoor background particles from the atmosphere were  
4 characterized; and (3) activity-based measurements: the sampling locations were selected based on  
5 information gathered and the walkthrough survey, considering factors such as air movement and  
6 currents, the work tasks, and whether they could allow for the placement of large instruments  
7 without affecting normal working activities. The sampling height of monitoring instruments for  
8 area sampling was close to the breathing zone of the workers. The timeline of the test protocol is  
9 summarized in Table 2.

### 17 **Data analysis**

20 One-way analysis of variance (ANOVA) was used for ER, together with the least significant  
21 difference (LSD) post hoc test (equal variances) or Dunnett's T3 post hoc test (unequal variances),  
22 to analyze differences between the three exposure metrics corresponding to different work  
23 locations and backgrounds. If there is a statistically significant difference between two groups in  
24 ANOVA analysis, the ER is considered to be different. Spearman correlation analysis was used to  
25 analyze correlations between respirable MC, NC, and lung deposited SAC.  
26  
27  
28  
29  
30  
31  
32  
33  
34

### 35 **Results**

#### 37 **Identification of particle nature**

40 Table 4 shows the chemical composition of different nanoparticles determined via EDX. The  
41 chemical composition of collected particles was significantly different from that of indoor or  
42 outdoor background particles. Some specific elements of each sample type were observed, such as  
43 Fe (29.70%) of Nano-Fe<sub>2</sub>O<sub>3</sub>, Al (60.91%) of Nano-Al<sub>2</sub>O<sub>3</sub>, S (1.84%) of diesel exhaust, Fe  
44 (16.10%) and Mn (2.46%) of welding particles, and Si (10.84%) and Fe (15.39%) of  
45 grinding-wheel dust. Table 5 shows higher-than-background levels of NC and lung deposited SAC  
46 of different particles at their corresponding work sites, as all ERs (activity: indoor background) of  
47 NC<sub>20-1000nm</sub> and lung deposited SAC<sub>10-1000nm</sub> were higher than 1.6.  
48  
49  
50  
51  
52  
53  
54  
55  
56  
57  
58  
59  
60

1  
2  
3  
4 Fig. 1 illustrates that size distributions by number were different from those (irregular shape)  
5  
6 of outdoor background environments. For instance, we observed bimodal distribution of  
7  
8 nano- $\text{Al}_2\text{O}_3$  or grinding-wheel dust, and unimodal distribution of nano- $\text{Fe}_2\text{O}_3$ , welding particles or  
9  
10 diesel exhaust. In addition, SEM analysis (Fig. 2) showed that spindle-like agglomerates of  $\text{Fe}_2\text{O}_3$   
11  
12 nanoparticles, cloud-like agglomerates of  $\text{Al}_2\text{O}_3$  nanoparticles, and chain-like agglomerates of  
13  
14 welding nanoparticles were quite different from the (irregular) morphology of indoor background  
15  
16 particles. The irregular and agglomerated morphology of grinding-wheel particles and diesel  
17  
18 exhaust particles also differed from that of background particles.  
19  
20  
21  
22

### 23 24 **Comparison of CR between three exposure metrics**

25  
26 Table 5 lists the CR of respirable  $\text{MC}_{100-1000\text{nm}}$ ,  $\text{NC}_{20-1000\text{nm}}$ , and lung deposited  $\text{SAC}_{10-1000\text{nm}}$   
27  
28 for different kinds of nanoparticles. The CR values of  $\text{NC}_{20-1000\text{nm}}$ , lung deposited  $\text{SAC}_{10-1000\text{nm}}$ ,  
29  
30 and respirable  $\text{MC}_{100-1000\text{nm}}$  of different nanoparticles were higher than 1.0, except in the case of  
31  
32 respirable  $\text{MC}_{100-1000\text{nm}}$  of  $\text{Fe}_2\text{O}_3$  or  $\text{Al}_2\text{O}_3$  nanoparticles at the packaging site. The CR values of  
33  
34  $\text{NC}_{20-1000\text{nm}}$ , lung deposited  $\text{SAC}_{10-1000\text{nm}}$  and of all types of nanoparticles were higher than for  
35  
36 respirable  $\text{MC}_{100-1000\text{nm}}$ . The mode size of different particles sampled ranged from 10.14–128.64  
37  
38 nm.  
39  
40  
41  
42

### 43 44 **Comparison of ER between three exposure metrics**

45  
46 Table 6 lists the ERs of  $\text{Al}_2\text{O}_3$  and  $\text{Fe}_2\text{O}_3$  nanoparticles at different work sites. The ER of  
47  
48  $\text{NC}_{20-1000\text{nm}}$  at different sites within the nano- $\text{Al}_2\text{O}_3$  manufacturer premises was ranked as follows:  
49  
50 outdoor background = control room (indoor background) < inlet of cold air < packaging; this was  
51  
52 identical to that of  $\text{SAC}_{10-1000\text{nm}}$  but not consistent with that of respirable  $\text{MC}_{100-1000\text{nm}}$ . The ER of  
53  
54  $\text{NC}_{20-1000\text{nm}}$  or  $\text{SAC}_{10-1000\text{nm}}$  for  $\text{Fe}_2\text{O}_3$  nanoparticles at different work sites was ranked as follows:  
55  
56  
57  
58  
59  
60

1  
2  
3  
4 outdoor background = indoor background < packaging < powder screening = material feeding,  
5  
6 differing from that of respirable  $MC_{100-1000nm}$ .  
7

### 8 **Comparison of APN and APM ratios**

9  
10 Table 7 demonstrates the ratio of APN and APM for  $Al_2O_3$  nanoparticles and grinding-wheel  
11 dust within similar size ranges. The APM of nano- $Al_2O_3$  particles smaller than 100 nm ( $D_a$ ) at the  
12 packaging location accounted for 44.24%, whereas the APN of nano- $Al_2O_3$  particles smaller than  
13 107.1 nm ( $D_a$ ) at the same location was 89.77%. The APM of grinding-wheel particles smaller  
14 than 100 nm ( $D_a$ ) at the polishing location accounted for 39.97%, whereas the APN of  
15 grinding-wheel particles smaller than 101.4 nm ( $D_a$ ) was 65.97%. The ratios of APN and APM for  
16 Nano- $Al_2O_3$  and grinding-wheel particles at the same work site were 2.03 and 1.65, respectively.  
17  
18  
19  
20  
21  
22  
23  
24  
25  
26  
27  
28

### 29 **Comparison of correlation coefficients between the three exposure metrics**

30  
31 Table 8 presents correlation coefficients (R) for the relationship between respirable  
32  $MC_{100-1000nm}$ ,  $NC_{20-1000nm}$ , and lung deposited  $SAC_{10-1000nm}$  for engineered nanoparticles or  
33 ultrafine particles. There was a strong correlation between  $NC_{20-1000nm}$  and lung deposited  
34  $SAC_{10-1000nm}$  (R=0.673 or 0.564,  $p<0.01$ ) for nano- $Fe_2O_3$  or nano- $Al_2O_3$ , and a moderate  
35 correlation between respirable  $MC_{100-1000nm}$  and lung deposited  $SAC_{10-1000nm}$  (R=0.271 or 0.366,  
36  $p<0.01$ ). However, the correlation between respirable  $MC_{100-1000nm}$  and  $NC_{20-1000nm}$  was  
37 inconsistent; that is, there was no correlation between respirable  $MC_{100-1000nm}$  and  $NC_{20-1000nm}$  for  
38 nano- $Fe_2O_3$  ( $p>0.05$ ) and a positive correlation for nano- $Al_2O_3$  ( $p<0.05$ ). Thus, no correlation  
39 between respirable  $MC_{100-1000nm}$  and  $NC_{20-1000nm}$  ( $p>0.05$ ) was found when the data for  
40 nano- $Fe_2O_3$  and nano- $Al_2O_3$  were combined for statistical analysis. With regard to ultrafine  
41 particles in workplaces, similar correlation coefficients to those of engineered nanoparticles were  
42  
43  
44  
45  
46  
47  
48  
49  
50  
51  
52  
53  
54  
55  
56  
57  
58  
59  
60

1  
2  
3  
4 observed between  $NC_{20-1000nm}$  and lung deposited  $SAC_{10-1000nm}$ , and respirable  $MC_{100-1000nm}$  and  
5  
6 lung deposited  $SAC_{10-1000nm}$ . The correlations between respirable  $MC_{100-1000nm}$  and  $NC_{20-1000nm}$  for  
7  
8 ultrafine particles were positive but relatively weak ( $R=0.183$ ). In general, the order of correlation  
9  
10 coefficients between the three exposure metrics for different kinds of nanoparticles was ranked as  
11  
12 follows:  $R_{SAC \text{ and } NC} > R_{SAC \text{ and } MC} > R_{NC \text{ and } MC}$ .

### 13 14 15 16 **Discussion**

17  
18 In this study, particle characteristics were identified by comparison with background particles  
19  
20 using four indices: total particle concentration, size distribution by number, chemical composition,  
21  
22 and morphology. The total concentration of different particles (especially in NC and lung  
23  
24 deposited SAC) at work sites involved in packaging, diesel combustion, welding, and high-speed  
25  
26 grinding was higher than respective indoor background levels, as their ERs were higher than 1.6.  
27  
28 Unimodal or bimodal size distributions of airborne particles differed from those (irregular shape)  
29  
30 of background particles. The average mode size of different particles sampled was less than 33 nm.  
31  
32 Further, the morphologies and elemental compositions of airborne particles were different from  
33  
34 those of the background particles. These findings indicate that airborne nanoparticles were indeed  
35  
36 released from different activities<sup>1,3</sup> and present specific particle characteristics. The three indices,  
37  
38 i.e. total particle concentrations (MC, NC and SAC), size distribution by number, and chemical  
39  
40 composition, have been used in previous field studies to identify the release of different  
41  
42 engineered nanoparticles (e.g. carbon nanotubes, nanoalumina, nanosilver, and nanoTiO<sub>2</sub>) during  
43  
44 production, handling and end-use stages.<sup>32-37</sup> Moreover, the number concentrations as determined  
45  
46 using a CPC or an OPC (optical particle counter), as well as morphology and elemental  
47  
48 composition, have been used as metrics by some international and national institutes for  
49  
50  
51  
52  
53  
54  
55  
56  
57  
58  
59  
60

1  
2  
3  
4 characterizing airborne nanoparticles.<sup>38-40</sup>  
5

6 Higher-than-background levels of NC and lung deposited SAC at the work sites (Table 5)  
7  
8 suggest that real-time NC and lung deposited SAC tests were better able to reflect actual levels of  
9  
10 exposure to nanoparticles in the workplace. Respirable  $MC_{100-1000nm}$  of nano- $Fe_2O_3$  released from  
11  
12 the packaging process was not significantly higher than background levels. The reason might be  
13  
14 that, with an average mode size of 12.26 nm, nano- $Fe_2O_3$  particles were not readily agglomerated  
15  
16 or aggregated into larger particles after surface treatment during the manufacturing process. Such a  
17  
18 nano-size particle does not interact strongly with electromagnetic radiation of optical wavelength,  
19  
20 and cannot be detected efficiently by a light-scattering photometer.<sup>41</sup> Three kinds of  $MC_{100-1000nm}$   
21  
22 for ultrafine particles generated at work sites were detected at relatively higher levels than the  
23  
24 corresponding background, although their CRs were obviously lower than those of  $NC_{20-1000nm}$  or  
25  
26  $SAC_{10-1000nm}$ . These results suggest that respirable MC, as a traditional exposure metric, may still  
27  
28 play a role in measuring exposure to nanoparticles, since such particles are more likely to be  
29  
30 agglomerated or aggregated into larger-size particles; however, the metric is not suitable for  
31  
32 measuring those airborne nanoparticles that are not readily agglomerated following certain surface  
33  
34 treatments. Furthermore, respirable  $MC_{100-1000nm}$  in this study was less sensitive to levels of  
35  
36 exposure to nanoparticles than were  $NC_{20-1000nm}$  or  $SAC_{10-1000nm}$ . This finding is supported by our  
37  
38 previous study, which demonstrated that respirable MC was not as sensitive as NC or SAC in  
39  
40 measuring nanoparticle levels at different welding points, sampling distances, and background  
41  
42 particles at an automobile manufacturing facility,<sup>22,42</sup> investigated incidental nanoparticles in an  
43  
44 engine machining and assembly facility, and found that the operation of direct-fire natural gas  
45  
46 heaters resulted in the greatest ultrafine particle concentrations without elevating respirable MC,  
47  
48  
49  
50  
51  
52  
53  
54  
55  
56  
57  
58  
59  
60

1  
2  
3  
4 indicating that respirable MC may not be a sensitive indicator of exposure to ultrafine particles.  
5

6 ER is an approach to identify similar exposure groups that may play a critical role in  
7  
8 epidemiological and exposure assessment.<sup>23,43</sup> In this study, higher ER means higher particle  
9  
10 concentrations at corresponding work sites. For example, the highest ER of  $NC_{20-1000nm}$  and lung  
11  
12 deposited  $SAC_{10-1000nm}$  for nano- $Al_2O_3$  was observed at the packaging location, suggesting that, of  
13  
14 all workers in this manufacturing workshop, packaging workers were exposed to the highest levels  
15  
16 of  $Al_2O_3$  nanoparticles (in  $NC_{20-1000nm}$  or lung deposited  $SAC_{10-1000nm}$ ) (Table 6). In addition, the  
17  
18 ER of  $NC_{20-1000nm}$  at different work locations within the nano- $Al_2O_3$  manufacturer site was the  
19  
20 same as that of lung deposited  $SAC_{10-1000nm}$ , but was not consistent with that of respirable  
21  
22  $MC_{100-1000nm}$ . Similar phenomena were observed for nano- $Fe_2O_3$ . These results indicate that the  
23  
24 perceived ER of different worker groups is highly dependent on the exposure metrics chosen. NC  
25  
26 or SAC may be a more sensitive exposure metric to classify similar worker groups exposed to  
27  
28 nanoparticles than respirable MC. These findings are supported by other related investigations.  
29  
30 Park *et al.*<sup>21</sup> compared ER by particle mass, number, and surface area concentrations in different  
31  
32 areas of a restaurant and a die-casting plant, and found that ERs based on NC and SAC in different  
33  
34 working areas were different from those for mass concentration. Ramachandran *et al.*<sup>23</sup>  
35  
36 investigated ERs of different job groups exposed to diesel exhaust, including bus drivers, bus  
37  
38 mechanics, and parking garage attendants, and found that the exposure groups presented quite  
39  
40 different ERs depending on the metrics chosen.  
41  
42  
43  
44  
45  
46  
47  
48  
49  
50

51 In the present study, the ratios of APN and APM for nano- $Al_2O_3$  and grinding-wheel particles  
52  
53 smaller than 100 nm at the same work site were 2.03 and 1.65 (Table 7) respectively, which  
54  
55 indicates that the number concentration of airborne nanoparticles was predominant in total number  
56  
57  
58  
59  
60

1  
2  
3  
4 concentration, whereas mass concentration accounted for only a small fraction of total mass  
5  
6 concentration. This result was in agreement with our previous study, which investigated workplace  
7  
8 exposure to nanoparticles from gas metal arc welding processes and found that welding  
9  
10 nanoparticles by number comprised 60.7% of particles, whereas welding nanoparticles by mass  
11  
12 accounted for only 18.2% of total particles.<sup>22</sup> These results, indicating that nanoparticles  
13  
14 contribute more to number concentration than mass concentration.  
15  
16  
17

18  
19 The relationship between MC, NC, and SAC is a focus of attention in most field studies on  
20  
21 nanoparticle exposure. In our study, it was clear that lung deposited SAC showed a high  
22  
23 correlation (R 0.558–0.673) with NC, and a moderate correlation (R 0.205–0.366) with respirable  
24  
25 MC for both engineered nanoparticles and ultrafine particles. A strong correlation between SAC  
26  
27 and NC was also reported by some field studies that focused on ultrafine particles, including those  
28  
29 generated from high-speed grinding, dry cutting, or combustion.<sup>20,23,32,44</sup> In a preliminary study on  
30  
31 workplace exposure to nanoparticles generated from a gas metal arc welding process, we found a  
32  
33 high degree of correlation between SAC and NC, and a relatively weak correlation between SAC  
34  
35 and respirable MC.<sup>22</sup> The high correlation found between NC and SAC could be related to the fact  
36  
37 that while the P-Track counts numbers of particles, the Aerotrak charges particles in a unipolar  
38  
39 charger and then measures the current that happens to be proportional to lung deposited SAC. In  
40  
41 general, there was a low correlation (R ranged from 0.097 to 0.248) between NC and respirable  
42  
43 MC for engineered nanoparticles or ultrafine particles. No positive correlation was observed  
44  
45 between NC and respirable MC for primary Fe<sub>2</sub>O<sub>3</sub> nanoparticles (average mode size of 12.26 nm)  
46  
47 with absence of agglomeration, suggesting that the smaller the particle, the more difficult it is to  
48  
49 detect it in mass concentration. This unstable correlation between NC and respirable MC for  
50  
51  
52  
53  
54  
55  
56  
57  
58  
59  
60

1  
2  
3  
4 engineered nanoparticles was also reported in several field studies. Demou *et al.*<sup>45</sup> carried out  
5  
6 25-day exposure measurement for airborne nanoparticles with mode size of 200 nm in a  
7  
8 production facility for metal-based nanomaterials, and found no correlation between MC (PM<sub>1.0</sub>)  
9  
10 and NC (up to 1.0 μm) during the majority of the sampling period, where MC failed to reflect the  
11  
12 manufacturing profile. Maynard *et al.*<sup>46</sup> also reported a lack of correlation between MC and NC  
13  
14 for single-wall carbon nanotube material during clean-up activity, as the variation in NC (rather  
15  
16 than MC) correlated closely with a vacuum cleaner. In contrast, several field studies reported a  
17  
18 positive correlation between MC and NC, especially for larger-size particles. During the  
19  
20 pelletizing process of carbon black, a good correlation was observed between MC and NC.<sup>47</sup>  
21  
22 Methner *et al.*<sup>48</sup> observed a similar increasing trend in both NC (larger than 400 nm) and MC  
23  
24 (PM<sub>10</sub>) that was associated with various handling processes of carbon nanofibers, such as transfer  
25  
26 and wet sawing. In the present study, the order of correlation between the three exposure metrics  
27  
28 for different nanoparticles was generally:  $R_{SAC \text{ and } NC} > R_{SAC \text{ and } MC} > R_{NC \text{ and } MC}$ . Evaluating the  
29  
30 biological relevance of an exposure-related metric is another way of determining its  
31  
32 appropriateness. Many toxicological studies have demonstrated that NC or SAC appeared to be  
33  
34 better exposure metrics than MC.<sup>13</sup> The unique characteristics of nanoparticles, such as increased  
35  
36 surface area, higher particle numbers per unit mass, and surface reactivity are considered to play  
37  
38 an important role in pronounced inflammatory response or greater oxidative stress in the  
39  
40 lungs.<sup>8,14,15,16, 49,50</sup>  
41  
42  
43  
44  
45  
46  
47  
48  
49  
50

51 It is necessary to reduce measurement error when using the P-trak ultrafine particle counter.  
52  
53 In a high concentration environment, this instrument can experience coincidence errors, i.e. more  
54  
55 than one particle can pass through the sensing region at a time, with these then counted as a single  
56  
57  
58  
59  
60

1  
2  
3  
4 particle<sup>51</sup>. This phenomenon starts to affect P-trak measurements at about 200,000 particles/cm<sup>3</sup>,  
5  
6 suggesting that the P-Trak may underreport nanoparticle number concentrations due to  
7  
8 coincidence errors.<sup>21</sup> Although NC at various work sites in this study was less than 200,000  
9  
10 particles/cm<sup>3</sup>, these coincidence errors should be noted. The use of a dilution system with the  
11  
12 P-Trak is able to decrease measurement error.<sup>52,53</sup> In addition, aerosol mass concentration is  
13  
14 determined using an aerosol photometer (DustTrak) based upon light scattering, which is strongly  
15  
16 affected by particle size and refractive index of photometer. Particles smaller than about 50 nm do  
17  
18 not interact strongly with electromagnetic radiation at optical or near optical wavelengths, and so  
19  
20 are not detected efficiently by light blocking or scattering.<sup>41</sup> The refractive index is strongly  
21  
22 material dependent and therefore the response of a photometer has to be calibrated for the specific  
23  
24 aerosol. Typically a photometer is calibrated for the average aerosol to be expected in a workplace  
25  
26 or the atmosphere. If particle properties deviate from the assumptions made in the calibration, the  
27  
28 results can be significantly biased.  
29  
30  
31  
32  
33  
34  
35

### 36 **Conclusions**

37  
38  
39 Several conclusions can be drawn from this analysis: (1) five kinds of nanoparticles were  
40  
41 released from different activities and have different respective particle characteristics; (2)  
42  
43 respirable MC was less sensitive than NC or SAC to levels of exposure to different nanoparticles,  
44  
45 but may still play a role in measuring exposure to those nanoparticles that are more likely to be  
46  
47 agglomerated or aggregated into larger-size particles; (3) NC or SAC may be a more sensitive  
48  
49 exposure metric than respirable MC for classifying similar worker groups exposed to  
50  
51 nanoparticles; (4) the NC of Al<sub>2</sub>O<sub>3</sub> and grinding-wheel nanoparticles was predominant as  
52  
53 compared with MC; (5) the order of correlation coefficient between the three exposure metrics for  
54  
55  
56  
57  
58  
59  
60

1  
2  
3  
4 nanoparticles was:  $R_{SAC \text{ and } NC} > R_{SAC \text{ and } MC} > R_{NC \text{ and } MC}$ . In general, NC and SAC metrics are  
5  
6 significantly distinct from MC in characterizing exposure to airborne nanoparticles. Simultaneous  
7  
8 measurement of NC, SAC, and MC should be conducted as part of nanoparticle exposure  
9  
10 assessment strategies and epidemiological studies.

11  
12  
13  
14 The present study has several practical implications. Particle characteristics that are  
15  
16 identified by comparison with background particles using multiple metrics, such as total particle  
17  
18 concentration, size distribution by number, chemical composition, and morphology, may be useful  
19  
20 for assessing whether airborne nanoparticles are released from different work activities. This study  
21  
22 provides the option of using multiple indices (such as CR (activity: background), ER,  
23  
24 between-metric correlation coefficients, and ratios of APN and APM) to analyze the relationship  
25  
26 between different exposure metrics. It is recommended that a combination of multiple metrics is  
27  
28 used as part of a well-designed sampling strategy for airborne nanoparticles. The set of baseline  
29  
30 exposure data for the five kinds of nanoparticles (especially for nano-Fe<sub>2</sub>O<sub>3</sub> and nano-Al<sub>2</sub>O<sub>3</sub>)  
31  
32 provided in this study can be used for further epidemiological investigation of nanoparticle-related  
33  
34 diseases. However, a few limitations of the study should be noted. Exposure data were obtained  
35  
36 using static measurements, and thus should be interpreted with care as estimates of personal  
37  
38 exposure. The results obtained from this field study regarding the relationship between the three  
39  
40 exposure metrics (NC, SAC, and MC) cannot conclude which exposure metric is most appropriate  
41  
42 or best. Moreover, these results are specific to the particles investigated and may not be widely  
43  
44 applicable to all nanoparticles, since characteristics such as particle morphology may change the  
45  
46 relationship between the measurements made by various instruments.  
47  
48  
49  
50  
51  
52  
53  
54  
55  
56  
57  
58  
59  
60

## Acknowledgements

We would like to thank Dr. Jipeng Cheng (Zhejiang University, China) for his technical support in connection with SEM and EDX analysis of nanoparticles.

This work was supported by the Natural Science Foundation of China (81472961); the Co-constructed Projects by the National Health and Family Planning Commission of China and the Health Bureau of Zhejiang Province (No. WKJ2014-ZJ-0 ); the Science and Technology Fund of the Health Bureau of Zhejiang Province, China (N0.2014KYB061; No.2012KYB050); the Innovation Projects of the Beijing Academy of Science and Technology (PXM2014-178304-000001-00130138) and the Innovation Teamwork Projects of the Beijing Academy of Science and Technology (IG201402C1); the Health Standards Fund of the Ministry of Health, China (20130215); The Science and Technology Project for Key Technology of Major Accident Prevention (Beijing-0003-2014AQ).

The authors declare that they have no financial or non-financial competing interests. The authors alone are responsible for the content and writing of the paper.

## Notes and references

<sup>a</sup> Zhejiang Provincial Center for Disease Control and Prevention, Hangzhou 310051, Zhejiang, People's Republic of China.

<sup>b</sup> Department of Environmental and Occupational Health Sciences, School of Public Health and Information Sciences, University of Louisville, Louisville, Kentucky, 40202, United States of America

<sup>c</sup> Beijing Municipal Institute of Labor Protection, Beijing 100054, People's Republic of China

\*\* Corresponding author. E-mail: mbzhang@cdc.zj.cn

\*Corresponding author. E-mail: tsc3496@sina.com

## References

- 1 ISO/TR 27628. 2007. Workplace atmospheres. Ultrafine, nanoparticle and nano-structured  
2 aerosols. Inhalation exposure characterization and assessment. Available from: www.iso.org  
3 (accessed 13 Nov 2008).
- 4 2 BSI PAS 71. 2008. Vocabulary. Nanoparticles, 2005. Available from: www.bsigroup.com/nano  
5 (accessed 13 Nov 2008).
- 6 3 J. H. Vincent and C. F. Clement, *Phil Trans R Soc Lond A.*, 2000, **358**, 2673–2682.
- 7 4 B. Fubini, M. Ghiazza and I. Fenoglio, *Nanotoxicology.*, 2010, **4**, 347–363.
- 8 5 M. R. Gwinn and V. Vallyathan, *Environ Health Perspect.*, 2006, **114**, 1818–1825.
- 9 6 K. Savolainen, H. Alenius, H. Norppa, L. Pylkkänen, T. Tuomi and G. Kasper, *Toxicology.*, 2010,  
10 **269**, 92–104.
- 11 7 N. Singh, B. Manshian, G. J. Jenkins, S. M. Griffiths, P. M. Williams, T. G. Maffei, C. J. Wright  
12 and S. H. Doak, *Biomaterials.*, 2009, **30**, 3891–3914.
- 13 8 D. M. Brown, M. R. Wilson, W. MacNee, W. Stone and K. Donaldson, *Toxicol Appl*  
14 *Pharmacol.*, 2001, **175**, 191–199.
- 15 9 D. M. Brown, N. Kanase, B. Gaiser, H. Johnston and V. Stone, *Toxicol Lett.*, 2014, **224**,  
16 147–156.
- 17 10 C. A. Dick, D. M. Brown, K. Donaldson and V. Stone, *Inhal Toxicol.*, 2003, **15**, 39–52.
- 18 11 C. A. Pope, R. T. Burnett, G. D. Thurston, M. J. Thun, E. E. Calle, D. Krewski and J. J.  
19 Godlesk, *Circulation.*, 2004, **109**, 71–77.
- 20 12 Q. Sun, A. Wang, X. Jin, A. Natanzon, D. Duquaine, R. D. Brook, J. S. Aguinaldo, Z. A. Fayad,  
21 V. Fuster, M. Lippmann, L. C. Chen and S. Rajagopalan, *JAMA.*, 2005, **294**, 3003–3010.
- 22 13 A. D. Maynard and R. J. Aitken, *Nanotoxicology.*, 2007, **1**, 26–41.
- 23 14 G. Oberdörster, *Phil Trans R Soc Lond A.*, 2000, **358**, 2719–2740.
- 24 15 T. Stoeger, C. Reinhard, S. Takenaka, A. Schroepel, E. Karg, B. Ritter, J. Heyder and H.  
25 Schulz, *Environ Health Perspect.*, 2006, **114**, 328–333.
- 26 16 C. L. Tran, D. Buchanan, R. T. Cullen, A. Searl, A. D. Jones and K. Donaldson, *Inhal Toxicol.*,  
27 2000, **12**, 1113–1126.
- 28 17 A. Nel, T. Xia, L. Madler and N. Li, *Science.*, 2006, **311**, 622–627.
- 29 18 D. Brouwer, *Toxicology.*, 2010, **269**, 120–127.

- 1  
2  
3 19 T.A. Kuhlbusch, C. Asbach, H. Fissan, D. Göhler, M. Stintz, *Part Fibre Toxicol.*, 2011, **8**,  
4 1-18.  
5  
6  
7 20 W. A. Heitbrink, D. E. Evans, B. K. Ku, A. D. Maynard, T. J. Slavin and T. M. Peters, *Occup*  
8 *Environ Hyg.*, 2009, **6**, 19–31.  
9  
10 21 J. Y. Park, G. Ramachandaran, P. C. Raynor and G. M. Olson, *J Occup Environ Hyg.*, 2010, **7**,  
11 466–476.  
12  
13 22 M. B. Zhang, L. Jian, P. F. Bin, M. L. Xing, J. L. Lou, L. M. Cong, H. Zou, *J Nanopart Res.*,  
14 2013, **15**, 2016–2030.  
15  
16 23 G. Ramachandran, D. Paulsen, W. Watts and D. Kittelson, *J Environ Monit.*, 2005, **7**, 728–735.  
17  
18 24 W. G. Kreyling, T. Tuch, A. Peter, M. Pitz, J. Heinrich, M. Stolzel, J. Cyrus, J. Heyder and H. E.  
19 Wichmann, *Atmos Environ .*, 2003, **37**, 3841–3848.  
20  
21 25 H. J. Jung, D. B. Kittelson, *Aerosol Sci Technol.*, 2005, **39**, 902-911  
22  
23 26 C. Asbach, H. Fissan , B. Stahlmecke, T. A. J. Kuhlbusch, D. Y. H. Pui, *J Nanopart Res.*, 2009,  
24 **11**, 101-109.  
25  
26 27 A. M. Keller, K. Fierz, H. Siegmann, C. Siegmann and A. Filippov, *J Vac Sci Technol.*, 2001,  
27 **19**, 1–8.  
28  
29 28 B. K. Ku and A. D. Maynard, *J Aerosol Sci.*, 2005, **36**, 1108-1124.  
30  
31 29 Y. H. Cheng, Y. C. Chao, C. H. Wu, C. J. Tsai, S. N. Uang and T. S. Shih, *J Hazard Mater.*,  
32 2008, **158**, 124-130.  
33  
34 30 H. Fissan, S. Neumann, A. Trampe, D. Y. H. Pui and W. G. Shin, *J Nanopart Res.*, 2007, **9**,  
35 53–59.  
36  
37 31 A. Khlystov, C. Stanier, and S. N. Pandis, *Aerosol Sci Tech.*, 2004, **38**, 229-238.  
38  
39 32 D. Bello, A. J. Hart, K. Ahn, M. Hallock, N. Yamamoto, E. Garcia, M. Ellenbecker and B.  
40 Wardle, *Carbon.*, 2008, **46**, 974–981.  
41  
42 33 D. Bello, B. L. Wardle, N. Yamamoto, D.R. Guzman, E. Garcia, A. Hart, K. Ahn, M.  
43 Ellenbecker and M. Hallock, *J Nanopart Res.*, 2009, **11**, 231–249.  
44  
45 34 T. A. J. Kuhlbusch, S. Neumann and H. Fissan, *J Occup Environ Hyg.*, 2004, **1**, 660–671.  
46  
47 35 J. H. Lee, M. Kwon, J. H. Ji, C. S. Kang, K. H. Ahn, J. H. Han and I. J. Yu, *Inhal Toxicol.*, 2011,  
48 **23**, 226–236.  
49  
50 36 S. J. Tsai, A. Ashter, E. Ada, J. L. Mead, C. F. Barry and M. J. Ellenbecker, *Aerosol Air Qual*  
51  
52  
53  
54  
55  
56  
57  
58  
59  
60

- 1  
2  
3  
4  
5  
6  
7  
8  
9  
10  
11  
12  
13  
14  
15  
16  
17  
18  
19  
20  
21  
22  
23  
24  
25  
26  
27  
28  
29  
30  
31  
32  
33  
34  
35  
36  
37  
38  
39  
40  
41  
42  
43  
44  
45  
46  
47  
48  
49  
50  
51  
52  
53  
54  
55  
56  
57  
58  
59  
60
- Res.*, 2008, **8**, 160–177.
- 37 S. J. Tsai, E. Ada, J. A. Isaacs, and M. J. Ellenbecker, *J Nanopart Res.*, 2009, **11**, 147–161.
- 38 J. H. Lee, J. Y. Lee and J. Yu, *Toxicol Res.*, 2011, **27**, 53–60.
- 39 NIOSH, 2009, DHHS (NIOSH) Publication No. 2009–125.
- 40 OECD, 2009, No. 11 ENV/JM/MONO (2009) 16.
- 41 L. Morawska, H Wang, Z. Ristovski, E. R. Jayaratne, G. Johnson, H. C. Cheung, X. Ling and C. He, *J Environ Monit.*, 2009, **11**, 1758–1773.
- 42 W. A. Heitbrink, D. E. Evans, T. M. Peters and T. J. Slavin, *J Occup Environ Hyg.*, 2007, **4**, 341–351.
- 43 J. Y. Park, G. Ramachandran, P. C. Raynor, L. E. Eberly and G. Olson, *Ann Occup Hyg.*, 2010, **54**, 799–812.
- 44 A. D. Maynard, *Ann Occup Hyg.*, 2003, **47**, 123–144.
- 45 E. Demou, P. Peter and S. Hellweg, *Ann Occup Hyg.*, 2008, **52**, 695–706.
- 46 A. D. Maynard, P. A. Baron, M. Foley, A. A. Shvedova, E. R. Kisin and V. Castranova, *J Toxicol Environ Health A* ., 2004, **67**, 87–107.
- 47 T. A. J. Kuhlbusch and H. Fissan, *J Occup Environ Hyg.*, 2006, **3**, 558–567.
- 48 M. M. Methner, M. E. Birch, D. E. Evan, B. K. Ku , K. Crouch and M. D. Hoover, *J Occup Environ Hyg.*, 2007, **4**, 125–130.
- 49 X. Y. Li, P. S. Gilmour, K. Donaldson and W. MacNee, *Thorax.*, 1996, **51**, 1216–1222.
- 50 V. Stone, J. Shaw, D. M. Brown, W. Macnee, S. P. Faux and K. Donaldson, *Toxicol In Vitro.*, 1998, **12**, 649–659.
- 51 K. Hameri, I. K. Koponen, P. P. Aalto and M. Kulmala, *J Aerosol Sci.*, 2002, **33**, 1463–1469.
- 52 L. D. Knibbs, R. J. de Dear, L. Morawska and P. M. Coote, *Atmos Environ.*, 2007, **41**, 4553–4557.
- 53 M. T. Peters, W. A. Heitbrink, D. E. Evans, T. J. Slavin and A. Marnard, *Ann Occup Hyg* 2006, **50**, 249–257.

## Figure legends

**Fig. 1** Size distributions of different nanoparticles determined via SMPS

**Fig. 2** Scanning electron micrographs of different airborne particles. **(a)** Irregular indoor background particles; **(b)** spindle-like agglomerates of  $\text{Fe}_2\text{O}_3$  nanoparticles collected at a packaging location; **(c)** cloud-like agglomerates of  $\text{Al}_2\text{O}_3$  nanoparticles collected at a packaging location; **(d)** syncretic agglomerates of diesel exhaust particles released from a forklift; **(e)** chain-like agglomerates of welding particles; **(f)** irregular agglomerates of grinding-wheel particles at a polishing location.

Table 1 Definitions of evaluation index terms

Term	Abbreviation	Definition	Related exposure metrics	Implication
Concentration ratio (activity: background)	CR	The ratio of total particle concentrations caused by various activities to concentrations at indoor background levels	Respirable MC, NC, and lung deposited SAC	To represent the sensitivity of different exposure metrics to concentration changes
Exposure ranking	ER	The ranking of different exposed groups based on statistical differences in metrics between two groups	Respirable MC, NC, and lung deposited SAC	To evaluate the accuracy with which each exposure metric reflects the real exposure profile
Cumulative percentage by number	APN	The percentage of particle number concentration within a specific size range (especially less than 100 nm) to cumulative number concentration within total size range	Size distribution by number	To analyze the percentage of nanoparticle number
Cumulative percentage by mass	APM	The percentage of particle mass concentration at a specific size range (especially less than 100 nm) to cumulative mass concentration within total size range	Size distribution by mass	To analyze the percentage of nanoparticle mass
Ratio of APN to APM	-	APN divided by APM	Size distribution by number and size distribution by mass	To analyze whether nanoparticle number is predominant in total particle number
Correlation coefficient	R	A measure of the strength of straight-line or linear relationships between two variables	Respirable MC, NC, and lung deposited SAC	To reflect the correlation extent of different exposure metrics

Table 2 General information regarding sampling locations

Factory	Sampling location	Reason for particle release	Particle control measure	Sampling date	Timeline of test protocol
Nano-Fe <sub>2</sub> O <sub>3</sub>	Indoor background	-	-	Oct 11 <sup>st</sup> -13 <sup>nd</sup> , 2012	6:30~7:30
	Powder screening	Manual screening of powder in open process	None		7:33~9:08
	Material feeding	Manual pouring of powder	Local exhaust hood		9:13~11:45
	Packaging	Semi-automatic packaging of powder	Dust extraction device		13:02~15:19
	Outdoor background	-	-		15:23~16:52
Nano-Al <sub>2</sub> O <sub>3</sub>	Cold air inlet	High pressure for air back-flushing in separator	General ventilation	May 27 <sup>th</sup> -29 <sup>th</sup> , 2013	9:04~11:46
	Packaging	Automatic packaging of powder in open process	Dust extraction device		12:10~15:32
	Control room (Indoor background )	-	-		15:52~16:25
	Outdoor background	-	-		16:35~17:52
Kitchenware	Indoor background	-	-	May 22 <sup>nd</sup> -24 <sup>rd</sup> , 2013	7:30~8:30
	Forklift	Diesel combustion	None		8:35~15:45
	Outdoor background	-	-		16:00~17:15
Elevator	Indoor background	-	-	May 24 <sup>th</sup> -26 <sup>th</sup> , 2013	6:40~7:40
	GMAW	Hot process	Dust extraction device		7:45~15:21
	Outdoor background	-	-		15:30~16:40
Foundry	Indoor background	-	-	Oct 16 <sup>th</sup> -18 <sup>th</sup> , 2012	6:10~7:10
	Polishing	High-speed mechanical process	Dustproof water-curtain		7:23~11:23
	Outdoor background	-	-		12:30~13:40

Table 3 Monitoring and sampling system for measuring particles

Monitoring type	Exposure metric	Instrument	Instrument type	Particle size	Measuring range	Sampling rate	log interval
Real-time monitoring	Total MC or respirable MC	DustTrak 8530 (TSI, USA)	Size integrated and time resolved	100~1000 nm	0.001~150 mg/m <sup>3</sup>	3 L/min	1 min
	Total NC	P-Trak 8525 (TSI, USA)	Size integrated and time resolved	20~1000 nm	0~500,000 particles/cm <sup>3</sup>	0.1 L/min	1 min
	Total SAC	Aero Trak <sup>TM</sup> 9000 (TSI, USA)	Size integrated and time resolved	10~1000 nm	1~10000 μm <sup>2</sup> /cm <sup>3</sup>	2.5 L/min	1 min
	Size distribution by number	SMPS 3034 (TSI, USA)	Size resolved and time resolved	10~487 nm	1~2.4×10 <sup>6</sup> particles/cm <sup>3</sup>	1.0 L/min	3 min
Membrane-based sampling	Size distribution by mass	Nano-MOUDI 125A (MSP, USA); Aluminum foil	Size resolved and time integrated	10~10000 nm	-	10.0 L/min	-
	Elemental composition	EDX (Hitachi, Japan)	-	10~10000 nm	-	-	-

MC: mass concentration; NC: number concentration; SAC: surface area concentration; SEM: scanning electron microscopy; EDX: energy dispersive X-ray spectroscopy.

Table 4 Chemical compositions of different nanoparticles

Work site	Particles	Constituent elements (% by mass)
Outdoor <sup>a</sup>	Ambient particulate	C (70.13), O (26.89), Na (0.87), Si (0.75), S (0.17), Fe (1.18)
Indoor <sup>a</sup>	Indoor background particles	C(63.83), O(29.77), Si(1.34), Fe(3.75), S(0.32), Na (0.99)
Packaging	Nano-Fe <sub>2</sub> O <sub>3</sub>	C (15.44), O (51.39), Na (1.34), Si (1.34), S (0.43), Ca (0.37), Fe (29.70)
Packaging	Nano-Al <sub>2</sub> O <sub>3</sub>	C (13.89), O (23.25), Al (60.91), Si (1.95)
Forklift	Diesel exhaust	C (76.93), O (20.41), Si (0.28), S (1.84), K (0.28), Ca (0.26)
GMAW	Welding particles	C (41.93), O (34.42), Si (3.39), Fe (16.10), Mn (2.46), Zn (0.80), Cu (0.90)
Polishing	Grinding-wheel dust	C (26.85), O (44.37), Na (1.07), Si (10.84), Fe (15.39), Mn (0.52), S (0.32), Ca (0.64)

GMAW: gas metal arc welding;

<sup>a</sup>: a representative chemical composition for indoor or outdoor background particles at different locations.

Table 5 Concentration ratios of respirable mass, number, and surface area concentrations for different kinds of nanoparticles

Factory	Work site	Particles	n <sup>a</sup>	Mode size (Range)	NC <sub>20–1000nm</sub> (10 <sup>4</sup> /cm <sup>3</sup> )		SAC <sub>10–1000nm</sub> (μm <sup>2</sup> /cm <sup>3</sup> )		MC <sub>100–1000nm</sub> (mg/m <sup>3</sup> )	
					Mean ± SD	CR	Mean ± SD	CR	Mean ± SD	CR
Nano-Fe <sub>2</sub> O <sub>3</sub> manufacturer	Packaging	Nano-Fe <sub>2</sub> O <sub>3</sub>	137	12.26±1.91 (10.37–17.15)	2.87±1.28	2.05	25.34±7.09	1.65	0.04±0.03	0.80
	Outdoor	Background	89	-	1.51±0.50		17.02±5.73		0.03±0.01	
	Indoor	Background	60	-	1.40 ±0.31		15.37 ±1.50		0.05 ± 0.01	
Nano-alumina manufacturer	Packaging	Nano-Al <sub>2</sub> O <sub>3</sub>	202	20.43±6.23 (13.85–35.23)	2.54±1.05	2.02	31.72±14.52	2.04	0.08±0.02	0.57
	Outdoor	Background	77	-	1.22±0.64		12.05±1.76		0.06±0.01	
	Indoor	Background	33	-	1.26±0.07		15.55±1.90		0.14±0.03	
Kitchenware	Forklift	Diesel exhaust	430	18.11±0.62 (13.96–30.53)	9.99±8.27	5.20	38.88±22.25	1.97	0.15±0.11	1.67
	Outdoor	Background	75	-	2.20±0.64		18.64±6.48		0.08±0.03	
	Indoor	Background	60	-	1.92±0.54		19.72±7.53		0.09±0.04	
Elevator	GMAW	Welding particles	536	32.99±28.93 (10.37–128.64)	10.32±4.47	4.04	185.11±58.76 <sup>a</sup>	5.19	0.32±0.05	1.45
	Outdoor	Background	70	-	1.87±0.71		29.49±9.38		0.12±0.04	
	Indoor	Background	60	-	2.55± 0.38		35.67 ± 10.50		0.22 ± 0.05	
Foundry	Polishing	Grinding-wheel dust	240	20.66±11.19 (10.14–58.29)	13.25±9.11	3.27	162.61±86.47 <sup>a</sup>	4.46	0.36±0.20	2.40
	Outdoor	Background	70	-	3.61±0.65		33.76±3.40		0.17±0.10	
	Indoor	Background	60	-	4.05 ±0.60		36.46±3.52		0.15 ±0.11	

CR: concentration ratio (activity: outdoor background); GMAW: gas metal arc welding;

<sup>a</sup>: the number of data points in a set of measurements.

Table 6 Exposure rankings of Al<sub>2</sub>O<sub>3</sub> and Fe<sub>2</sub>O<sub>3</sub> nanoparticles at different work sites

Nanoparticle	Work site	n <sup>a</sup>	NC <sub>20-1000nm</sub> (10 <sup>4</sup> /cm <sup>3</sup> )		SAC <sub>10-1000nm</sub> (μm <sup>2</sup> /cm <sup>3</sup> )		MC <sub>100-1000nm</sub> (mg/m <sup>3</sup> )	
			Mean ± SD	ER	Mean ± SD	ER	Mean ± SD	ER
Nano-Al <sub>2</sub> O <sub>3</sub>	Packaging	202	2.54±1.05	3	31.72±14.52	3	0.08±0.02	1
	Cold air inlet	162	2.21±1.08	2	24.88±6.05	2	0.10±0.02	2
	Control room	33	1.26±0.07	1	15.55±1.90	1	0.14±0.03	3
	Outdoor background	77	1.22±0.64	1	14.86±1.55	1	0.07±0.01	1
Nano-Fe <sub>2</sub> O <sub>3</sub>	Packaging	137	2.87±1.28	2	22.20±7.50	2	0.04±0.02	1
	Powder screening	95	5.04±1.39	3	26.21±4.38	3	0.05±0.04	1
	Material feeding	152	6.68±2.02	3	29.54±9.1	3	0.26±0.10	2
	Indoor background	60	1.40 ±0.31	1	15.37 ±1.50	1	0.05 ± 0.01	1
	Outdoor background	89	1.51±0.50	1	14.11±1.64	1	0.04±0.01	1

NC: number concentration; SAC: surface area concentration; MC: mass concentration; ER: exposure ranking;

<sup>a</sup>: the number of data points in a set of measurements.

1  
2  
3  
4  
5  
6  
7  
8  
9  
10  
11  
12  
13  
14  
15  
16  
17  
18  
19  
20  
21  
22  
23  
24  
25  
26  
27  
28  
29  
30  
31  
32  
33  
34  
35  
36  
37  
38  
39  
40  
41  
42  
43  
44  
45  
46  
47  
48  
49

Table 7 Size distribution by mass and by number for Al<sub>2</sub>O<sub>3</sub> nanoparticles and grinding-wheel dust

Work site	Particles	Size distribution by mass			Size distribution by number				Ratio (APN: APM)
		Size range (D <sub>a</sub> , nm)	AC (mg/m <sup>3</sup> )	APM (%)	Size range (D <sub>p</sub> , nm)	Size range (D <sub>a</sub> , nm)	AC (10 <sup>4</sup> /cm <sup>3</sup> )	APN (%)	
Packaging	Nano-Al <sub>2</sub> O <sub>3</sub>	10~56	0.0667	32.18	10~54.2	11.1~60.2	1.04	73.55	2.29
		57~100	0.0917	44.24	54.3~96.5	60.3~107.1	1.27	89.77	2.03
		101~320	0.1240	59.82	96.6~327.8	107.2~363.9	1.40	98.94	1.65
		321~560	0.2073	100.00	327.9~469.8	364.0~521.5	1.42	100.00	1
Polishing	Grinding-wheel dust	10~56	0.0261	11.96	10~35.2	16.2~57.0	4.38	38.16	3.19
		57~100	0.0870	39.97	35.3~62.5	57.1~101.4	7.57	65.97	1.65
		101~320	0.1305	59.98	62.6~198.1	101.5~320.9	10.96	95.54	1.59
		321~560	0.2174	100.00	198.2~352.3	321.0~570.7	11.47	100.00	1

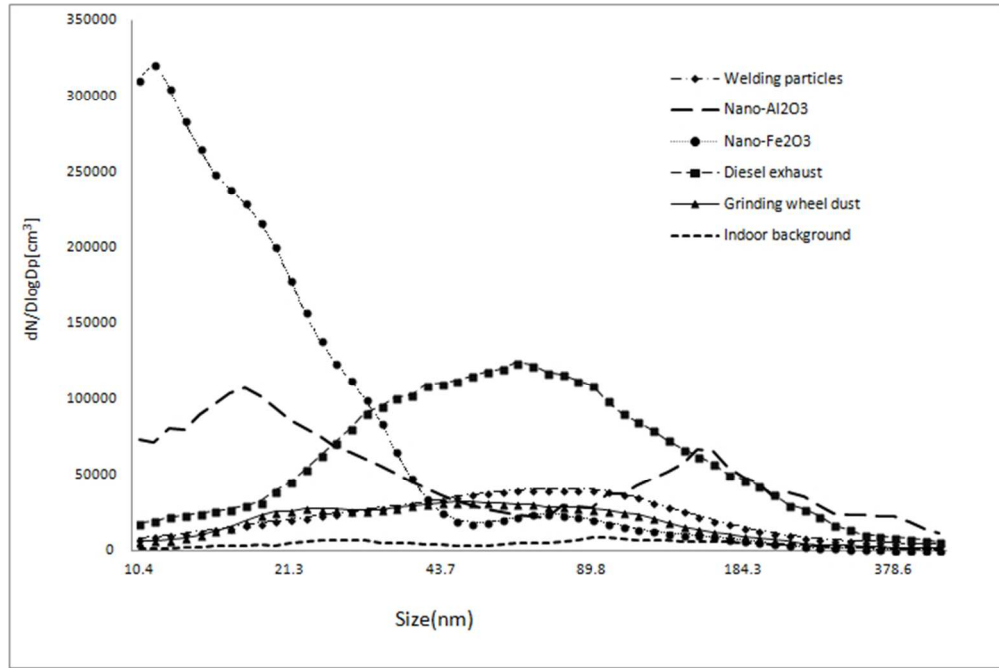
AC: cumulative concentration; APM: cumulative percentage by mass; APN: cumulative percentage by number; D<sub>a</sub>: aerodynamic diameter; D<sub>p</sub>: mobility diameter.

For example, APM (44.24 %) of less than 100 nm particles is calculated from AC (0.0917) of 57~100 nm particles divided by that of 321~560 nm particles.

Table 8 Correlation coefficients of mass, number and surface area concentrations (n=2110)

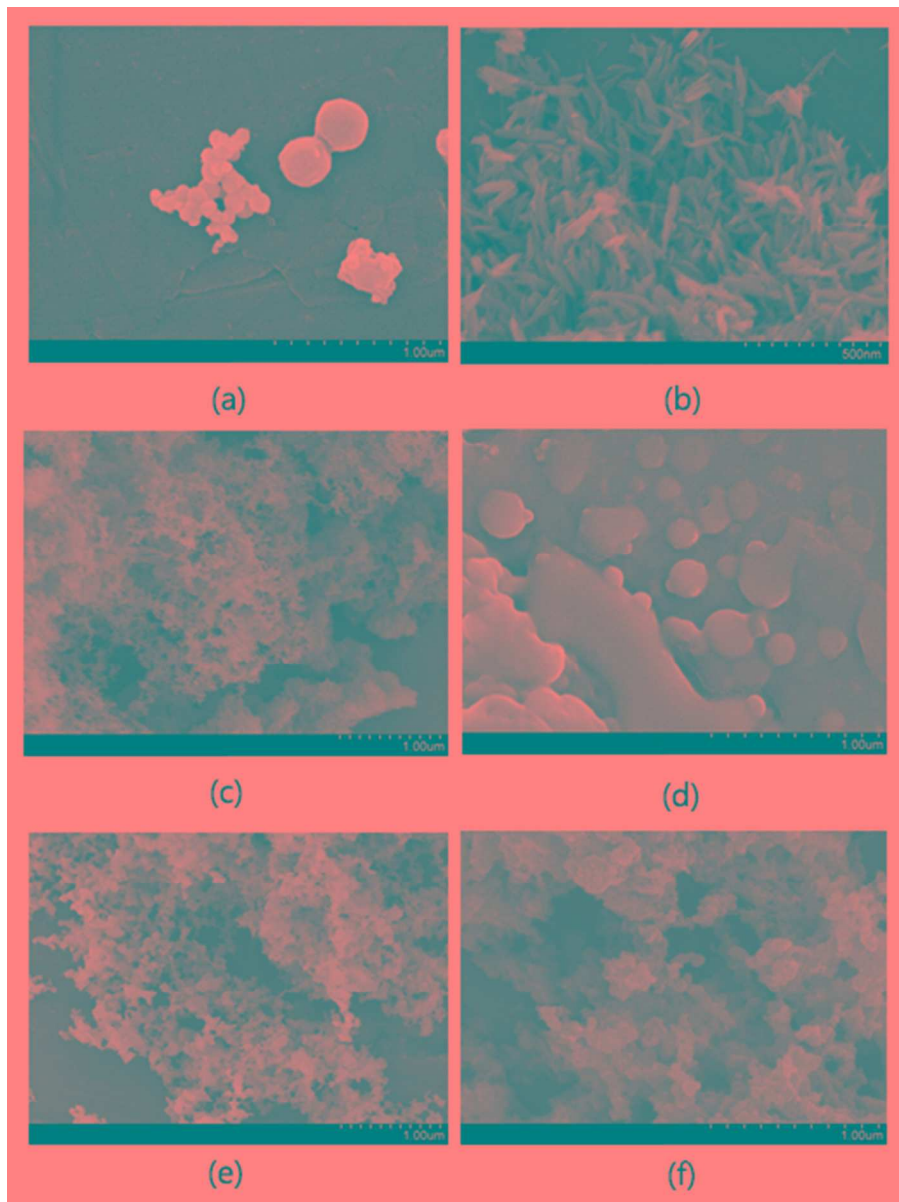
Particles	n	Metrics	MC <sub>100-1000nm</sub>	NC <sub>20-1000nm</sub>	SAC <sub>10-1000nm</sub>
Nano-Fe <sub>2</sub> O <sub>3</sub>	366	MC <sub>100-1000nm</sub> (mg/m <sup>3</sup> )	1.00	-	-
		NC <sub>20-1000nm</sub> (10 <sup>4</sup> /cm <sup>3</sup> )	0.097	1.00	-
		SAC <sub>10-1000nm</sub> (μm <sup>2</sup> /cm <sup>3</sup> )	0.271 <sup>a</sup>	0.673 <sup>b</sup>	1.00
Nano-Al <sub>2</sub> O <sub>3</sub>	512	MC <sub>100-1000nm</sub> (mg/m <sup>3</sup> )	1.00	-	-
		NC <sub>20-1000nm</sub> (10 <sup>4</sup> /cm <sup>3</sup> )	0.210 <sup>a</sup>	1.00	-
		SAC <sub>10-1000nm</sub> (μm <sup>2</sup> /cm <sup>3</sup> )	0.366 <sup>a</sup>	0.564 <sup>b</sup>	1.00
Engineered nanoparticles	878	MC <sub>100-1000nm</sub> (mg/m <sup>3</sup> )	1.00	-	-
		NC <sub>20-1000nm</sub> (10 <sup>4</sup> /cm <sup>3</sup> )	0.157	1.00	-
		SAC <sub>10-1000nm</sub> (μm <sup>2</sup> /cm <sup>3</sup> )	0.329 <sup>a</sup>	0.628 <sup>b</sup>	1.00
Diesel exhaust	480	MC <sub>100-1000nm</sub> (mg/m <sup>3</sup> )	1.00	-	-
		NC <sub>20-1000nm</sub> (10 <sup>4</sup> /cm <sup>3</sup> )	0.192 <sup>a</sup>	1.00	-
		SAC <sub>10-1000nm</sub> (μm <sup>2</sup> /cm <sup>3</sup> )	0.210 <sup>a</sup>	0.558 <sup>b</sup>	1.00
Welding particles	445	MC <sub>100-1000nm</sub> (mg/m <sup>3</sup> )	1.00	-	-
		NC <sub>20-1000nm</sub> (10 <sup>4</sup> /cm <sup>3</sup> )	0.248 <sup>a</sup>	1.00	-
		SAC <sub>10-1000nm</sub> (μm <sup>2</sup> /cm <sup>3</sup> )	0.252 <sup>a</sup>	0.609 <sup>b</sup>	1.00
Grinding-wheel dust	307	MC <sub>100-1000nm</sub> (mg/m <sup>3</sup> )	1.00	-	-
		NC <sub>20-1000nm</sub> (10 <sup>4</sup> /cm <sup>3</sup> )	0.186 <sup>a</sup>	1.00	-
		SAC <sub>10-1000nm</sub> (μm <sup>2</sup> /cm <sup>3</sup> )	0.205 <sup>a</sup>	0.647 <sup>b</sup>	1.00
Ultrafine particles	1232	MC <sub>100-1000nm</sub> (mg/m <sup>3</sup> )	1.00	-	-
		NC <sub>20-1000nm</sub> (10 <sup>4</sup> /cm <sup>3</sup> )	0.183 <sup>a</sup>	1.00	-
		SAC <sub>10-1000nm</sub> (μm <sup>2</sup> /cm <sup>3</sup> )	0.241 <sup>a</sup>	0.588 <sup>b</sup>	1.00
Total	2110	MC <sub>100-1000nm</sub> (mg/m <sup>3</sup> )	1.00	-	-
		NC <sub>20-1000nm</sub> (10 <sup>4</sup> /cm <sup>3</sup> )	0.169 <sup>a</sup>	1.00	-
		SAC <sub>10-1000nm</sub> (μm <sup>2</sup> /cm <sup>3</sup> )	0.279 <sup>a</sup>	0.605 <sup>b</sup>	1.00

<sup>a</sup>  $p < 0.05$ ; <sup>b</sup>  $p < 0.01$



188x125mm (96 x 96 DPI)

1  
2  
3  
4  
5  
6  
7  
8  
9  
10  
11  
12  
13  
14  
15  
16  
17  
18  
19  
20  
21  
22  
23  
24  
25  
26  
27  
28  
29  
30  
31  
32  
33  
34  
35  
36  
37  
38  
39  
40  
41  
42  
43  
44  
45  
46  
47  
48  
49  
50  
51  
52  
53  
54  
55  
56  
57  
58  
59  
60



137x183mm (96 x 96 DPI)

1  
2  
3  
4  
5  
6  
7  
8  
9  
10  
11  
12  
13  
14  
15  
16  
17  
18  
19  
20  
21  
22  
23  
24  
25  
26  
27  
28  
29  
30  
31  
32  
33  
34  
35  
36  
37  
38  
39  
40  
41  
42  
43  
44  
45  
46  
47  
48  
49  
50  
51  
52  
53  
54  
55  
56  
57  
58  
59  
60